



# SRI International

Year-End Technical Report 1 • October 1992

## ADVANCED ELECTRONIC STRUCTURES

Mark van Schilfgaarde, Research Physicist  
Physical Electronics Laboratory

SRI Project 2407

Prepared for:

Office of Naval Research  
800 North Quincy Street  
Arlington, Virginia 22207

Attn: Dr. Larry R. Cooper

Contract N00014-19-C0139

DTIC  
ELECTE  
DEC 08 1992  
S A D


This document has been approved  
for public release and sale; its  
distribution is unlimited.

## CONTENTS

1.	INTRODUCTION .....	1
2.	STUDIES UNDERTAKEN DURING THE PAST YEAR .....	1
2.1	Schottky Barriers and Defects .....	1
2.2	Fullerene $\text{Ti}_8\text{C}_{12}$ .....	2
2.3	InTISb as an Infrared Detector .....	3
2.4	Magnetic Multilayers .....	5
2.5	Defects in $\text{HgCdTe}$ .....	6
3.	METHODS .....	7
3.1	Progress .....	7
3.2	Current and Planned Work .....	9

  
**92-30899**  
 1298

Accession For	
NTIS CRA&I	<input checked="" type="checkbox"/>
DTIC TAB	<input type="checkbox"/>
Unannounced	<input type="checkbox"/>
Justification	
By <i>per ltr</i>	
Distribution/	
Availability Codes	
Dist	Avail and/or Special
A-1	

**92-29285**  


## 1. INTRODUCTION

This is the first year-end technical report on Contract N00014-91-C0139, covering the period March 1991 through February 1992. The results of the studies undertaken during the year are described first, along with discussions of current work in progress (Section 2). Section 3 describes the methods used and the progress made in developing effective ways of addressing these interesting problems. Appended are preprints and reprints of papers reporting the results of several of the studies.

## 2. STUDIES UNDERTAKEN DURING THE PAST YEAR

### 2.1 SCHOTTKY BARRIERS AND DEFECTS

#### 2.1.1 Progress

This work, undertaken with Nathan Newman and Eike Weber of U.C. Berkeley, was reported in a short talk at the March 1992 meeting of the American Physical Society. The subject was the use of *pressure* as a new variable for testing the underlying mechanism governing Schottky barrier height. Eike Weber showed that, when properly interpreted, the pressure dependence of the Pt/GaAs barrier height matched the pressure dependence of the *isolated antisite* defect. Shortly after the March meeting, I completed a series of calculations complementing these findings. The calculated pressure dependence of the isolated antisite defect agrees very well with the measured dependence, once corrected as Eike showed. This confirmation was very satisfying. Next, the pressure dependence of the barrier height of an ideal Pt/GaAs Schottky barrier was calculated. Its pressure dependence with respect to the valence band was found to have the opposite sign from what was found experimentally. However, the calculated pressure dependence of a Schottky barrier with an As antisite defect near the interface closely tracks the pressure dependence of the antisite itself, as it must on electrostatic grounds. Thus, when the Schottky barrier has a reasonably high density of antisite defects near the interface, the barrier height follows the experimentally observed pressure dependence; without the antisite defect, the calculated pressure dependence deviates significantly from what is observed. We find this result a very persuasive argument in favor of the defect model, and believe it casts serious doubt on the MIGS model. We intend to submit to *Physical Review Letters*, and are only waiting for Eike to complete a draft of the manuscript.

### 2.1.2 Current Work

We are beginning to collaborate in two other arenas. One concerns the growth of GaN as a potential candidate for a wide-bandgap laser. Being a sturdy, III-V compound, GaN may offer an attractive candidate for a wide-bandgap semiconductor for laser applications. Dr. Newmann has set up machine at Lawrence Berkeley Laboratory to grow GaN and has made some intriguing observations about the N defects in that material. It appears that, because N<sub>2</sub> is so stable as a molecule, there is a stronger tendency to form anion vacancies than is customary in III-V materials. I am complementing his work with calculations of a number native defects important in GaN.

Miguel Samaron's group at LBL is well known for its STM work; and Drs. Newman and Weber have a collaborative project with him. Part of Dr. Samaron's program includes scattering calculations that simulate experimental studies. So far, they have used tight-binding calculations for these models, and so I have been invited to work jointly with them to attempt similar studies, from the point of view of *ab initio* methods. This collaboration has just begun, so there is little to report yet.

### 2.2 FULLERENE Ti<sub>8</sub>C<sub>12</sub>

This work is a collaboration with M. Methfessel of the Max Planck Institute in Germany. Very recently Guo, Kerns, and Castleman<sup>1</sup> discovered a new cluster with a stoichiometry Ti<sub>8</sub>C<sub>12</sub>. Further, they were able to determine that the eight Ti atoms were all equivalent, which led them to propose the structure shown in Figure 1, next page. Using our newly completed molecules program (see below) we studied this molecule to determine whether the proposed structure is likely to be correct, and what its bonding properties are. As in C<sub>60</sub>, all atoms in this "soccerball-shaped" molecule are threefold coordinated; here, however, only five-fold rings occur. Furthermore, the surface is more strongly curved and consequently the corresponding fullerene C<sub>20</sub> is *not* stable.

Starting with the structure in the figure and adding small random displacements, we carried out a molecular-dynamics simulation to relax the structure to its minimum energy configuration. The results confirm the structure, although the dodecahedron deforms, with the C-C bond length shrinking to 1.39 Å and the Ti-C bond increasing to 1.99 Å. The calculated binding energy was huge in view of the low coordination number—6.61 eV per atom. For comparison, the binding energy of the diamond comes out to approximately 5.5 eV/atom, and we calculate the LDA binding energy of TiC in the NaCl structure—known to be an extremely hard material—to be 7.16 eV/atom.

By studying the electronic wave functions and the charge density, we have analyzed the bonding. The Fermi energy lies between the bonding and nonbonding states, explaining the stability of the cluster. However, contrary to expectations, no analog to the graphitic bonding in the C<sub>60</sub> molecule is found. Bonding in graphite is due to (1) σ bonding of localized and strongly directed *sp*<sup>2</sup> orbitals which point to the three neighbors; (2) π bonding among the *p*<sub>z</sub> orbitals perpendicular to the plane. Neither of these two mechanisms can be identified; rather, we find that the electronic structure should be thought of as a C<sub>2</sub> dimer, which combines with the Ti *d* orbitals to make bonding cluster states. The bonding of a Ti atom to its three carbon neighbors is through these *d* orbitals which, owing to their special shape, have the flexibility to adapt to the shape of

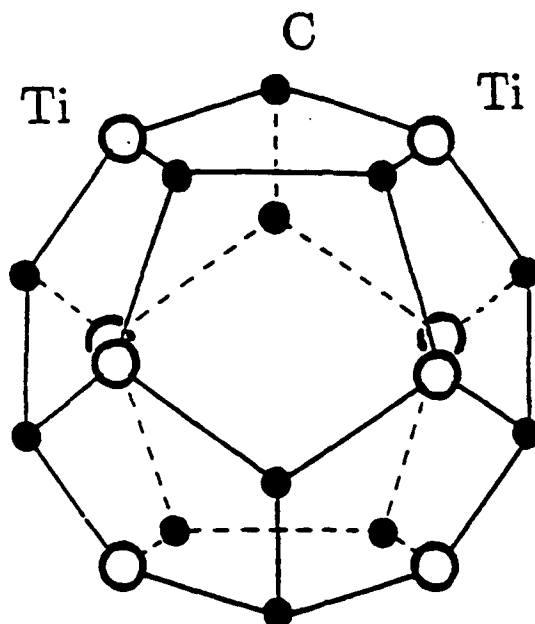


Figure 1. Proposed structure of TiC cluster

the  $C_2$  molecular orbitals. Because the bonding is so dissimilar to the graphitic-like bonding in  $C_{60}$ ,  $Ti_8C_{12}$  should be considered as belonging to a completely different class of molecular clusters. In the first four bands, 42 bonding states are available, which are filled almost completely by the 80 valence electrons; this explains the exceptional stability of this cluster. However it also indicates that a similar cluster in which Ti substituted for an earlier or later transition metal would be less stable. We recently submitted the enclosed manuscript to *Physical Review Letters*.

### 2.3 InTiSb as AN INFRARED DETECTOR

This work was undertaken with Arden Sher of SRI. It occurred to us that by alloying Ti into InSb, the bandgap of the host might be narrowed just as the gap of CdTe narrows when alloyed with Hg. Provided Ti is miscible into InSb, the resulting compound should be far more robust than HgCdTe, and thus more viable as an LWIR detector. This is so first because III-V compounds are generally more robust than II-VIs and also because InSb is already a narrow-gap material, unlike CdTe. Thus for a 0.1-eV bandgap TiInSb would require only a small amount of Ti, while in HgCdTe the larger, weaker Hg predominates. This difference was the motivation for making a detailed study of the alloy. We calculated, within the local density-functional approximation, a host of electronic and structural properties of InSb, TiSb, and InTiSb in the zinc blende structure. Fortunately, the errors the LDA makes are fairly small and quite systematic; by adjusting for these errors, we are able to predict the electronic and structural data with a high degree of confidence, provided TiInSb can really be grown in that structure.

Our calculated bond length in InSb came out to 2.80 Å, about 0.5% smaller than the observed 2.81 Å; the calculated bond length in TiSb came out to 2.85 Å. The resulting 2% bond length mismatch is quite good—only slightly worse than that of HgCdTe—and the strain energy of the InTiSb alloy is small. Indeed, we found essentially no tendency to spinodally decompose

if the nuclei are confined to the zinc blende lattice. The calculated bandgap of TlSb (adjusting for systematic LDA errors) was found to be  $-1.5$  eV. The origin of this strongly negative gap can be traced largely to a pronounced deepening of the Tl  $s$  state from relativistic corrections to the Schrödinger equation. (A similar phenomenon takes place in HgTe, which explains why its gap is so much smaller than that of CdTe.) Since the gap of InSb is approximately  $0.3$  eV, only about 10% Tl is needed to make a  $0.1$ -eV gap. Also, the cohesive energy of TlSb was found to be  $1.2$  eV/bond, about 85% of the  $1.4$  eV found for InSb. These energies are to be compared with  $0.8$  and  $1.1$  eV for HgTe and CdTe, respectively. The calculations thus quantify and confirm our intuition that only a small amount of Tl is needed, and that  $\text{In}_{1-x}\text{Tl}_x\text{Sb}$  with  $x = 0.1$  will be far more robust than  $\text{Hg}_{1-x}\text{Cd}_x\text{Te}$  with  $x$  a comparable value. Figure 2 shows that the band structure of  $\text{In}_{1-x}\text{Tl}_x\text{Sb}$  looks quite similar to that of  $\text{Hg}_{1-x}\text{Cd}_x\text{Te}$  near  $\Gamma$ .

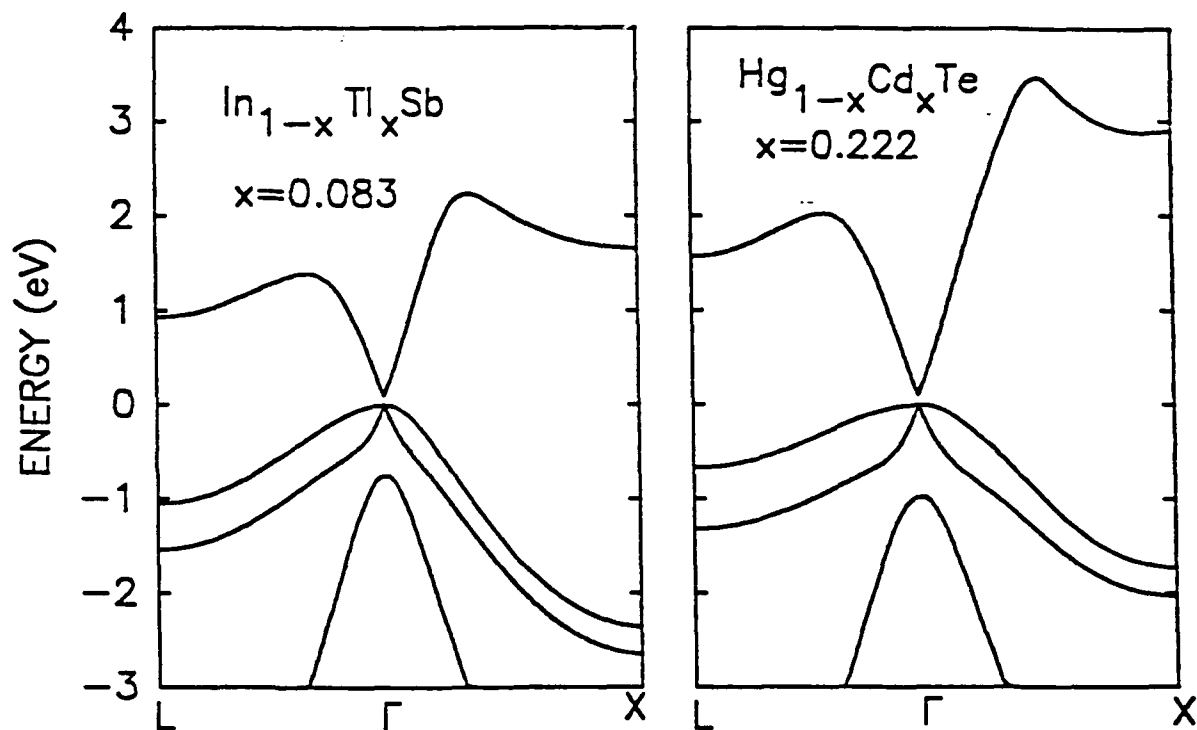


Figure 2. Comparison of HgCdTe with InTiSb

Unfortunately, there is a major complication, which we also studied in detail. Because of its strongly negative gap, TlSb was found to slightly favor the CsCl structure to the zinc blende (ZB); indeed the observed crystal structure of TlSb is CsCl. Beyond some critical composition  $x^*$ ,  $\text{InTiSb}$  will then decompose into a two phase region of  $\text{InSb}_x(\text{ZB})$  and  $\text{TlSb}_{1-x}(\text{CsCl})$ . Beyond  $x^*$ , then,  $\text{In}_{1-x}\text{Tl}_x\text{Sb}$  is worthless in electronic applications. We determined  $x^*$  by calculating the phase diagram of  $\text{In}_{1-x}\text{Tl}_x\text{Sb}$ . This was done with a regular solution model, and the total energies of  $\text{InSb}(\text{ZB})$ ,  $\text{InSb}(\text{CsCl})$ ,  $\text{TlSb}(\text{ZB})$  and  $\text{TlSb}(\text{CsCl})$ , which were obtained from careful density-functional calculations.

It turns out that InSb strongly favors the ZB structure to the CsCl while TlSb only slightly favors the CsCl structure to the ZB. This crucial point saves the day, and the resulting phase diagram (see the figure in the preprint) shows a modest amount of Tl (up to about 15%) can indeed

be incorporated into InSb in the ZB structure at temperatures of about 500 K. It must be cautioned that the phase diagram is not all that reliable, since it necessitated comparing very small energy differences between completely different crystal structures. On the other hand, I have recalculated some of these numbers using newly incorporated gradient corrections to the LDA, and the energy differences come out similarly. Thus we believe this calculated phase diagram approximates the true one reasonably well.

We find these early results very encouraging. The enclosed manuscript was submitted to *Applied Physics Letters*. One other important observation emerges from the calculated phase diagram.  $\text{In}_{1-x}\text{Tl}_x\text{Sb}$  cannot be grown from a liquid phase, because there is no path to the stable phase that bypasses a two-phase region. Thus  $\text{In}_{1-x}\text{Tl}_x\text{Sb}$  must be grown by some vapor phase technique.

## 2.4 MAGNETIC MULTILAYERS

### 2.4.1 Progress

This work is being carried out in collaboration with Frank Herman of IBM Almaden. We are studying the process by which a superlattice composed of a ferromagnetic (FM) metal sandwiched between a few atomic layers of a nonmagnetic spacer, such as Cu, can produce a giant magnetoresistance. Since this property can be exploited for magnetic recording applications it is of considerable technological interest. The large magnetoresistance occurs only when adjacent slabs of Fe are aligned antiferromagnetically. Application of a small magnetic field realigns all the slabs into a ferromagnetic arrangement, and produces a large change in the scattering at the spacer/magnet interface. Because the alignment must be antiferromagnetic (AFM) for the large magnetoresistance, the question of whether alignment is ferro- or antiferromagnetic is the central one. It turns out that the alignment oscillates between FM and AFM ordering as the nonmagnetic spacer thickness increases!

Until recently, there was no consensus regarding the origin of the interaction that governed the coupling of adjacent slabs. Whether the coupling was associated with an RKKY-like interaction, mediated by the nonmagnetic spacer, or some exotic many-body interaction was a much debated subject. By doing self-consistent density-functional calculations, we obtained oscillatory behavior in the several systems, most extensively the CoCu and FeCr systems. This showed fairly decisively that the effect is indeed due to an RKKY-like interaction. Actually, it is a greatly distorted RKKY interaction because it depends so strongly on details of the Fermi surface of the spacer layer. Fermi surfaces of transition metals or Cu look very different from each other and do not at all resemble free-electron bands, as the RKKY theory assumes. This is not a problem for us, since we are not doing the calculation in perturbative way, but instead solve the problem directly for a specific geometry. This automatically incorporates complexities of the band structure or any dependence on other details, such as any contribution to the coupling from the special boundary conditions at the magnet/spacer interface.

In the CoCu case, we observed oscillatory coupling, the period depending on the orientation of the interface. With the data we had it was fairly easy to resolve a short period for the [001] and [011] directions of about 4.2 to 4.4 Å, which is in quite fair agreement with the observed 4.6 Å. The data also show a second, longer period of approximately 15 Å, although

they do not yet extend far enough out to resolve this precisely. A second, longer period of 13 to 14 Å has been found experimentally on the [001]. Along the [111], we find a period of about 8 Å, a little smaller than the observed 11 to 12 Å. On the whole, agreement is remarkably good, considering that the energies involved here are only a few meV and that we are comparing calculations on idealized interfaces with those on real interfaces, with their warts and blemishes.

#### 2.4.2 CURRENT WORK

While these calculations show fairly definitively that the interactions are RKKY-like, and that first-principles LDA calculations can obtain quantitative agreement with experiment, they are heavy and tedious, and they need to be repeated for every new geometry. Because the energy differences are so small, and the magnetic moments converge slowly, often several hundreds of iterations are needed, each with thousands of  $k$  points, before we obtain a converged result. I have almost completed adapting a simplified, non-self-consistent procedure based on the Harris functional and O.K. Andersen's "tight-binding" representation of the LMTO orbitals. Applying this to the magnetic interface problem will give us the simplicity of a Harrison-like tight-binding picture, with an accuracy approaching that of fully self-consistent LDA calculations. With this in place, we can easily study a wide range of problems. We plan, for example, to study the effects of much longer range interactions and to study the effects of nonidealities at the interface, such as the relaxations there, or the rôle the intermixing of the interfacial atoms plays in reducing the coupling strength.

We are very optimistic about this approach, first because of its simplicity and also because we have the more complete, precise calculations as a standard to control the adequacy of approximations.

#### 2.5 DEFECTS IN HgCdTe

This work is being carried out in collaboration with Martha A. Berding of this laboratory. Dr. Berding has invested considerable effort in the study of point defects in the HgZnTe and HgCdTe alloys. Together, we employed density functional calculations to obtain the energetics of these defects and local relaxations. For my part, this fits in nicely with a larger plan to study point defects in III-V semiconductors with Eike Weber. We have obtained defect energies for a host of neutral native defects in CdTe, ZnTe and HgTe, including relaxations, and have studied to lesser degree the Fermi level dependence of these defects. In addition to the internal energy of the defect, which density-functional theory supplies, we obtain the free energy by calculating the entropy as well. I believe we can lay claim to being the first to render complete calculations of the free energy and equilibrium populations of defects from first principles, with no adjustable parameters. In agreement with experimental observations, we find excess Te predominantly takes the form of Hg vacancies when equilibrated with a Hg vapor. We also find that Hg anti-sites may be more prevalent than previously thought. By including the mass action equations for the many reactions that might take place between the solid and gas, we obtained electron and hole concentrations as a function of temperature (see the IRIS preprint). These last results do involve one or two parameters, such as the temperature variation of the band gap. As might be expected, the concentrations are extremely sensitive to small changes in these parameters, and to



the defect energies. Changes in energy on the order of  $kt$  produce large changes in these concentrations. In view of this, the agreement with experiment Dr. Berding obtains is quite satisfactory (see figure, IRIS preprint).

### 3. METHODS

#### 3.1 PROGRESS

All of the studies mentioned above hinge on the ability to perform electronic structure calculations. Michael Methfessel and I set out to build a new electronic structure program based on a principle quite different from anything attempted before. Indeed, this has consumed far more of our time than anything else in the past two years. We seem to have conquered the worst obstacles; our new method is showing some fruit, as the TiC paper shows. The following describes in a very brief sketch the main idea.

In any self-consistent method of calculating electronic structure, the researcher always faces three obstacles: (1) given a representation of the electron density, to solve for the potential; (2) generating the Hamiltonian from the potential; (3) generating the output density from the eigenvectors of the Hamiltonian. Only with a plane-wave (PW) method are all these steps straightforward; a PW method has drawbacks, however. It works well with smooth pseudopotentials only; a large number of PW are needed for any problem since they are not tailored to the potential of interest; and finally, the PW extend over all space. I believe that the state-of-the-art electronic structure method of the future must work with a local basis, since in a broad sense, interactions are spatially local. In large-scale applications, where density functional methods clearly are headed, it will matter a great deal whether the orbitals in the basis can be confined spatially to the interaction of interest, or whether orbitals of the basis extend everywhere in space. If they extend everywhere, the method necessarily must include all states in the system simultaneously, even though almost all of them are not relevant. Thus the famous  $N^3$  bottleneck is inevitable for an extended basis, meaning that the number of operations needed to carry out the linear algebra needed to solve the Schrödinger equations must scale as the third power of the size of the system. In principle the operations time need only scale linearly with the system size, since interactions are not of infinite range. This indicates in a general way that extended basis sets are ultimately less potent than local ones for large systems.

The drawback of a real-space method is that it is far more complicated. The three obstacles mentioned must be reckoned with. The first can be handled, provided that the electron density is represented by functions that are also eigenfunctions of the Poisson equation. The last obstacle entails the casting of wave function *products* as a *linear* sum of functions used to represent the charge density. In general, this is not possible analytically. We tackled the difficulty by doing the next best thing, which is to determine such a relation through a least-squares fit, and then tabulate the information so that any product can be recast into a sum via a lookup table. The tricky part was to retain the information in a compact way. This we accomplished by tabulating

a fit along the  $z$  axis, which can be represented compactly, and applying rotation matrices when needed for an arbitrary geometry. This solves Steps (2) and (3) at the same time, since hamiltonian matrix elements can be generated through the same lookup procedure.

We wrote a molecules program first, since that is most natural to a real-space method. We have tested it quite carefully now and are confident we have overcome the numerical troubles that plagued us for so long. The difficulties arose from controlling small but rapidly oscillating errors in the initial least-squares fit (which, amazingly enough, the usual computer machine precision was not quite sufficient to damp out). We have found ways to avoid this problem, and the program now works very well. Table 1 (some of which was presented at the March meeting) shows that the program can obtain good results—essentially identical to Soler's APW calculations for  $\text{H}_2\text{O}$ .

**Table 1**  
**Comparison of Structural Properties in Selected Molecules.**

$\theta$  are bond angles and  $\omega$  are vibrational frequencies.

Molecule	d (au)		E (eV)		$\theta$ (deg)		$\omega$ ( $\text{cm}^{-1}$ )	
	Calc	Expt	Calc	Expt	Calc	Expt	Calc	Expt
$\text{N}_2$	2.074	2.076	11.49	9.8		—	2380	2360
(Soler)	2.07		11.5				2400	
(Painter)	2.08		11.33					
$\text{H}_2$	1.444	1.410	4.91	4.5		—	4200	4400
(Painter)	1.45		4.91					
$\text{Cu}_2$	4.14		2.97	2.1		—	300	330
(Painter)	4.10		2.64					
$\text{H}_2\text{O}$	1.833	1.811	11.54	9.5	104.2	104.5	1650, 3770	1600, 3760
(Soler)	1.83		11.6		102.4		1610, 3670	
$\text{H}_2\text{S}$	2.564	2.543	8.95	7.5	91.2	92.3		
$\text{H}_2\text{Se}$	2.805	2.779	8.28		90.1	91.0		

We have obtained a novel expression for the forces in a general framework, and now have used it to implement a molecular-dynamics molecules program that simultaneously iterates on self-consistency with nuclear motion. Our theorem is quite different from the usual Hellman-Feynman theorem, and allows us to take much larger time steps than does the Car-Parrinello method. The  $\text{TiC}$  cluster mentioned above was relaxed using a dynamics algorithm. The main

body of a short paper describing the forces is enclosed; a completed version should be done quite soon. A longer paper describing the real-space method itself will also be written soon.

Since we are solid-state physicists, we are really more interested in a crystal program than in a molecules program. To this end, a preliminary version of a crystals program adapted from the molecules program has been completed. At this early stage, it works most of the time, but sometimes exhibits instabilities similar to the molecules program in its early stages. Fortunately we should know how to treat it now.

### **3.2 CURRENT AND PLANNED WORK**

Our first priority is to complete the crystal program and eliminate the instabilities. Once complete, our immediate goal is to find an alternative technique that solves for the eigenvalues, exploiting the real-space nature of the hamiltonian, just as the Car-Parrinello method really amounts to little more than a trick that exploits properties of plane waves to obtain eigenstates of the hamiltonians efficiently in that basis. I have hit upon a scheme which reduces the  $N^3$  bottle-neck to an  $N^2$  one, and discussed it in some detail with Beresford Parlett. He is a professor at Berkeley, and a renowned expert on the linear eigenvalue problem. He liked the idea and offered some variants, and we are likely to collaborate on this project. I find this quite exciting, since this really opens the possibility of opening the door to the next generation of electronic-structure methods.

If there is continued interest in discovering the forces of a free atom approaching a semiconductor surface, studying relaxations of free surfaces. With forces available to us, we should be able to address these issues now.

# Electronic structure and bonding in the metallic fullerene $\text{Ti}_8\text{C}_{12}$

M. Methfessel <sup>(1)\*</sup>, M. van Schilfgaarde <sup>(2)</sup>,  
and M. Scheffler<sup>(1)</sup>

<sup>(1)</sup>*Fritz-Haber-Institut der Max-Planck-Gesellschaft,  
Faradayweg 4-6, D-1000 Berlin 33, Germany*

<sup>(2)</sup>*SRI International, 333 Ravenswood Ave., Menlo Park,  
California 94025, U.S.A.*

(Received September 7, 1992)

Total-energy and electronic-structure calculations are presented for a recently-proposed dodecahedral cluster of eight titanium and twelve carbon atoms. The calculations were done using density-functional theory and a recently-developed cluster full-potential linear muffin-tin orbital method which is suited to arbitrary geometries and permits direct evaluation of the forces. As in the  $\text{C}_{60}$  molecule, the atoms form a spherical graphite-like shell with a three-fold coordination at all sites. The C-C and Ti-C bond lengths are calculated to be of 2.63 and 3.76 bohr, respectively, and the binding energy is 6.6 eV per atom. The bonding mechanism is quite different from that which stabilizes the graphite crystal or the  $\text{C}_{60}$  molecule.

36.40.td, 31.20.Sy, 61.50.Lt

Typeset Using *REVTeX*

Since the first observation of the  $C_{60}$  molecule [1], much effort has been invested in the study of this novel molecular cluster. In  $C_{60}$ , the carbon atoms form a hollow sphere consisting of 5-fold and 6-fold rings, whereby each atom has a coordination number of three. It can be considered a spherical form of graphite and it has been shown that the bonding mechanism is essentially the same. A short time ago, Guo, Kerns, and Castleman [2] discovered an unusually stable charged cluster with the stoichiometry  $Ti_8C_{12}$ . Furthermore, they were able to show that the eight Ti atoms are equivalent. For neutral and ionized molecules of this type (named metallo-carbohedrenes) they proposed the structure displayed in Fig. 1. The atoms are arranged at the corners of a dodecahedron with six  $C_2$  dimers alternating with the eight Ti atoms. As in  $C_{60}$ , all atoms in this "soccerball-shaped" molecule are three-fold coordinated; however, here only five-fold rings occur. Furthermore, the surface is more strongly curved and consequently the corresponding fullerene  $C_{20}$  is not stable. Interestingly, Ti can form a metastable  $\omega$  phase which has been interpreted as partly covalent[3]. The question thus arises whether the proposed structure is correct and, if yes, to what extent the bonding mechanism in this carbon-titanium molecule is analogous to that in the carbon fullerenes. To shed light on this question, we have performed ab-initio electronic structure calculations for  $Ti_8C_{12}$  in the proposed geometry. The results confirm the structure, whereby the dodecahedron is deformed somewhat due to the different lengths of C-C and Ti-C bonds. By studying the electronic wave functions and the charge density, we have analysed the bonding. We find that the electronic structure can be understood as  $C_2$  molecular orbitals combining with the Ti  $d$  orbitals to make bonding cluster states. The Fermi energy lies between the bonding and nonbonding states, explaining the stability of the cluster. No analog to the graphitic bonding in the  $C_{60}$  molecule is found, showing that indeed  $Ti_8C_{12}$  is a member of a new class of molecular clusters.

The calculations were done using a recently-developed full-potential linear muffin-tin orbital (FP-LMTO) method which is designed for clusters, to be presented in detail elsewhere[4]. The basis for the representation of the electronic eigenstates consists of atom-centered spherical Hankel functions which are augmented by numerical solutions of the radial Schrödinger equation inside non-overlapping atomic spheres. The combination of the augmentation technique with the use of LCAO-like atom-centered envelope functions leads to a very efficient basis set which can be applied to heavy and light elements equally well. As has been discussed previously [5], the main difficulty for a full-potential method using this basis set is to find a useable representation for the product of two such functions in the interstitial region (between the atomic spheres). As before, we represent these products as linear combinations of other atom-centered Hankel functions. In the new method, we first obtain an arbitrarily accurate such representation for pairs of atoms arranged along the  $z$  axis. The expansion coefficients are tabulated as function of the interatomic distance. For any other geometry, we obtain the needed expansion rapidly by evaluating the tabulated fit and applying rotation matrices. The electron-electron interaction is treated by the local-density approximation (LDA) [6,7] within density-functional theory; hereby the interstitial exchange-correlation quantities are obtained by numerical integration. In addition, it has been possible to derive an exact and practicable force theorem within this technique. In sum, the applied FP-LMTO method has these desirable features: (1) it can be applied to any cluster geometry (without the use of "empty spheres" or shape approximations to the density or potential); (2) it can be made arbitrarily accurate by increasing the precision of the initial pair-wise fit; (3) the forces on the nuclei are available. Tests for typical molecules such as  $N_2$ ,  $CO_2$ ,  $H_2O$ ,  $H_2S$ , and  $H_2Se$  yield results in very good agreement with experiment (except for the typical overbinding due to the LDA) as well as previous state-of-the-art calculations where

available.

In the present case, the muffin-tin radii were chosen 2.20 and 1.25 bohr for Ti and C, respectively. LMTO's of kinetic energies  $-0.4$ ,  $-1.0$ , and  $-2.0$  Ry were used with angular momentum cutoffs of  $l_{\max}=2, 2, 1$  on Ti and  $2, 1, 1$  on C, making a basis of 380 functions in total. The charge-density basis consisted of Hankel functions with kinetic energies  $-1$ ,  $-3$ ,  $-9$ , and  $-12$  Ry with angular momentum cutoffs of  $l_{\max}=3, 6, 3, 1$  on Ti and  $3, 4, 3, 1$  on C. Inside the spheres, the density and potential were expanded in spherical harmonics up to angular momentum  $l_{\max}=3$ . To speed up convergence, occupation numbers for the eigenstates were calculated using a gaussian broadening of 0.02 Ry. It was found necessary to treat the high-lying Ti 3s and 3p levels with the same accuracy as the valence states by means of a "two-panel" technique.

The proposed dodecahedral structure can be viewed as a cube of Ti atoms, with one C<sub>2</sub> dimer associated with each face. Symmetry operations are mirrors on the  $xy$ ,  $yz$ , and  $zx$  planes as well as the three-fold rotations around the cube diagonals, generating a symmetry group of 24 elements. To calculate the equilibrium structure, the atoms were placed on the corners of an ideal dodecahedron with small random displacements to break the symmetry. While iterating to self-consistency, the atoms were moved to follow the forces until these were smaller than 0.01 Ry/bohr. In the relaxed structure, the symmetry is recovered and the C-C bond length has contracted to 2.63 bohr while the Ti-C bond has expanded to 3.76 bohr. The C and Ti atoms have almost the same distance from the cluster center, namely 4.92 and 4.95 bohr, respectively. The charge density for the valence states is displayed in Fig. 2. The calculated binding energy is 6.61 eV per atom, taking into account spin-polarization energies of respectively 0.71 and 1.20 eV for the free Ti and C atoms. For comparison, the binding energy per atom for crystalline TiC in the NaCl structure is only slightly

larger at 7.16 eV (calculated using the technique of Ref. [5]), despite the twice as large coordination number. In summary, our calculation finds the distorted dodecahedral geometry stable and strongly bound for  $\text{Ti}_8\text{C}_{12}$ .

When Guo et al. proposed the dodecahedral structure for  $\text{Ti}_8\text{C}_{12}$ , they made the reasonable suggestion that the bonding mechanism is similar to that of graphite and  $\text{C}_{60}$ . As first ingredient they postulated a network of Ti-C and C-C  $\sigma$  bonds, involving  $d$ - $sp$  hybrids on the Ti atoms. Second, " $\pi$ -bonding" states made from metal  $d_\pi$  and carbon  $p_\pi$  orbitals were assumed to take up the remaining electrons. The transition metal is assigned a relevant role in stabilizing the molecule by reducing the strain, due to the strong curvature, which would make a hypothetical  $\text{C}_{20}$  molecule unstable. This model would place 30 valence electrons into the  $\sigma$  bonding and 10 electrons into  $\pi$  bonding states.

Our calculations support a somewhat different view of the electronic structure. We find that a more appropriate description is that of well-defined  $\text{C}_2$  dimers whose orbitals bind with the nearest-neighbor Ti  $d$  orbitals. To support this view, Fig. 3 shows the density of states for  $\text{Ti}_8\text{C}_{12}$ . There are four well-separated "bands" below the Fermi energy  $\epsilon_F$ . These correlate with the energy levels of the isolated  $\text{C}_2$  dimer (calculated at the same interatomic distance as in the cluster), also shown. A Mullikan projection onto the LMTO basis set was used to decompose the density of states into site and angular-momentum contributions[8]. The two lowest bands, containing six cluster states each, are mainly of C  $s$  character with a small amount of  $p$  character along the C-C bond mixed in. These are derived from the  $\text{C}_2$  bonding and antibonding  $\sigma$  states ( $1\sigma_g$  and  $1\sigma_u$  in Fig. 3). The third band (18 states) is in the same energy range as the  $p$ -like bonding states in the dimer ( $1\pi_u$  and  $2\sigma_g$  in Fig. 3). Finally, the band just below  $\epsilon_F$  (of which ten states are occupied) can be associated with the two dimer antibonding molecular orbitals,  $1\pi_g$ . The number of states in each band is



obtained correctly by multiplying the dimer molecular orbital degeneracies with the number of dimers in the cluster (six). This classification of the cluster eigenstates is clearly visible in the partial charge densities and wavefunctions (Fig. 4). In the cluster,  $C_2$  dimer states are occupied which are unoccupied in the free dimer. This indicates a transfer of charge from the Ti to the C atoms, in agreement with the electronegativities. The four bands are of 90, 70, 70, and 40% carbon character, respectively. In total, we obtain valence charges of 4.36 on the carbon and 3.46 on the titanium atoms, *i.e.*, a charge transfer of about 0.4 electrons per atom.

The bonding between carbon neighbors is due to the first three bands. Bonding between Ti and C atoms has some contributions from the second and third bands but is mainly due to the fourth band. Figure 5 illustrates how Ti-C bonding states can be made incorporating the  $C_2$  antibonding  $\pi$  states in a geometry with five-fold rings. These states weaken the C-C bonds to some extent. The unoccupied states above the Fermi energy are of practically pure Ti character and would not contribute to the bonding of the molecule if they were occupied. The energy range of this nonbonding band overlaps slightly with the fourth band. In total, there are  $6 + 6 + 18 + 12 = 42$  bonding states available in the first four bands. They are filled almost completely by the 80 valence electrons. Since the Fermi level falls between the bonding and nonbonding states, the cluster is exceptionally strongly bound. We conclude that a similar cluster with an earlier or later transition metal in place of Ti would be less stable. Interesting possibilities however open up if, in addition, some C atoms are replaced by neighbors in the periodic table, keeping the total number of valence electrons close to 80. The isoelectronic metal Zr and Hf are of course obvious candidates for a stable cluster of the same type as  $Ti_8C_{12}$ .

All cluster eigenstates have definite  $\sigma$  or  $\pi$  character along the C-C bond. Is it possible to classify the Ti-C bonds in the same way? The Ti  $d$  orbitals which could

participate hereby must be compatible with the  $C_{3v}$  point symmetry at a Ti site. The arrangement of the three C neighbors is essentially a tetrahedral coordination with a missing fourth corner atom. For this symmetry it is possible to define combinations of the  $d$  orbitals which are directed along the nearest neighbor bonds. However, inspection of the 40 occupied eigenstates did not yield a generally valid picture of well-defined Ti-C  $\sigma$  bonding. Similarly, no well defined Ti-C  $\pi$  bonds can be identified. To understand this, it is important to realize that the  $C_2$  dimer forms a very strong unit in the cluster. The  $C_2$  molecular orbitals, which force their shape onto the cluster wavefunctions, are at unusual angles relative to the Ti-C bond. An essential ingredient to the binding is the flexibility of the  $d$  orbitals which makes it possible to "hook together" these functions into bonding cluster states. Of the total valence charge on the Ti atoms, only 4.5% and 3.9% is associated with the  $s$  and  $p$  orbitals, respectively. Thus, it is essentially only the Ti  $d$  orbitals which participate in the bonding with carbon.

Nevertheless, it might be tempting to try to re-interpret our picture of the bonding as a graphite-like mechanism. This could be fueled by the fact that the number of states in the three lower bands (30) equals the number of possible bonding combinations of the  $sp^2$ -like orbitals from 20 atoms. However, this approach does not seem useful. Bonding in a graphite layer is understood to be due to two main contributions: (1)  $\sigma$  bonding of localized and strongly directed  $sp^2$  orbitals which point to the three neighbors; (2) additional  $\pi$  bonding due to the  $p_z$  orbitals perpendicular to the plane. Neither of these two mechanisms can be identified in our calculated results. We conclude that the bond of a Ti atom to its three carbon neighbors is clearly distinct from the bonding in graphite.

In summary, our ab-initio DFT-LDA calculation for the  $Ti_8C_{12}$  molecule in the dodecahedral structure obtains a stable and strongly bound geometry. The dodec-

ahedron is distorted somewhat because the C-C bonds are shorter compared to the Ti-C interatomic distance. The electronic structure can be understood as well-defined  $C_2$  dimers whose molecular orbitals combine with the Ti  $d$  functions to make bonding cluster wavefunctions. Charge transfer from Ti to C of about 0.4 electrons per atom fills  $C_2$  dimer states which are unoccupied in the free dimer. The Ti-C bonding is largely due to those cluster wavefunctions which are derived from the dimer antibonding  $p_\pi$  combinations. The Fermi energy lies between the bonding states and non-bonding Ti states, explaining the stability of the cluster. Overall, we find no significant similarity to the bonding mechanism which stabilizes graphite and the  $C_{60}$  molecule.

## REFERENCES

• Permanent address: Institut für Halbleiterphysik, Walter-Korsing-Str. 2, O-1200 Frankfurt/Oder, Germany.

- [1] H. W. Kroto, J. R. Heath, S. C. O'Brien, R. F. Curl, and R. E. Smalley, *Nature* **318**, 162 (1985); R. F. Curl and R. E. Smalley, *Science* **242**, 1017 (1988).
- [2] B. C. Guo, K. P. Kerns, and A. W. Castleman, Jr., *Science* **255**, 1411 (1992).
- [3] J. M. Sanchez and D. de Fontaine, *Phys. Rev. Lett.* **35**, 227 (1975).
- [4] M. Methfessel and M. van Schilfgaarde (unpublished).
- [5] M. Methfessel, *Phys. Rev. B* **38**, 1537 (1988); M. Methfessel, C. O. Rodriguez, and O. K. Andersen, *Phys. Rev. B* **40**, 2009 (1989).
- [6] P. Hohenberg and W. Kohn, *Phys. Rev.* **136**, B864 (1964); W. Kohn and L. J. Sham, *Phys. Rev.* **140**, A1133 (1965).
- [7] D. M. Ceperly and B. J. Alder, *Phys. Rev. Lett.* **45**, 566 (1980).
- [8] V. Fiorentini, M. Methfessel, and M. Scheffler, submitted to *Phys. Rev. B*. Note that the decomposition projects onto the atom-centered basis functions and not onto the angular momenta inside the spheres; thus the partial charges depend only weakly on the sphere radii and there is no separate interstitial contribution. Angular momenta are relative to local coordinate systems on the Ti and C atoms with the  $z$  axis pointing out of the cluster.

## FIGURES

FIG. 1. Possible structure of the  $\text{Ti}_8\text{C}_{12}$  molecule, as proposed in Ref. [2].

FIG. 2. Calculated valence charge density in a pentagonal face. The lowest contour and the contour spacing are 0.01 and 0.02 electrons/bohr<sup>3</sup>, respectively. Small discontinuities are due to the muffin-tin spheres.

FIG. 3. Density of states for the  $\text{Ti}_8\text{C}_{12}$  molecule. Eigenvalues were broadened by gaussians of width 0.01 Ry. The energy levels of the non-magnetic free C and Ti atoms and of the  $\text{C}_2$  dimer (with the same distance as in  $\text{Ti}_8\text{C}_{12}$ ) are also shown.

FIG. 4. Plots in a pentagonal face of a typical wavefunction (left) and the summed electron density (right) for each of the four occupied bands. For the third band, the shown wavefunction is of  $1\pi_u$  character on the  $\text{C}_2$  dimer; others of  $2\sigma_g$  character exist in the same band. Shown are the interstitial functions extended smoothly into the muffin-tin spheres. First contour and contour spacing are 0 and 10 for wavefunctions and 2.5 and 5.0 for densities in units of  $10^{-3}$  bohr<sup>-3</sup>. Negative contours are dashed, contour for zero is dotted.

FIG. 5. Sketch of the way in which the Ti  $d$  orbitals combine with the  $\text{C}_2$  dimer antibonding  $p_\pi$  wavefunctions to make bonding cluster wavefunctions. The carbon atom at the top is a member of another  $\text{C}_2$  dimer not in the plane of the paper.

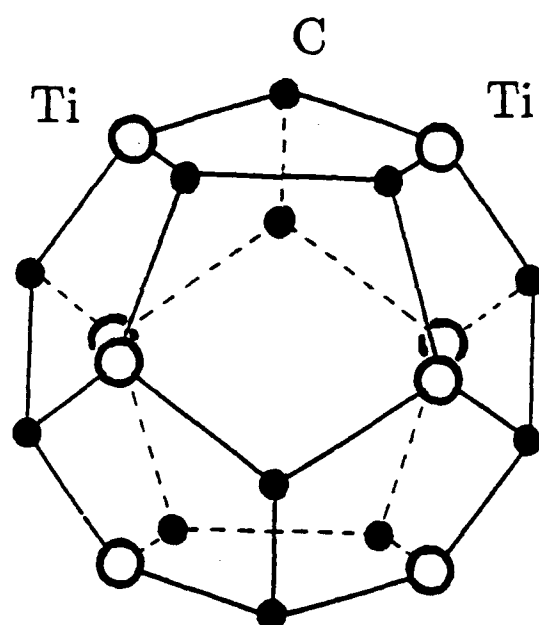


Fig. 1

PRL, Messfasser, Sch. 48000, schaffte

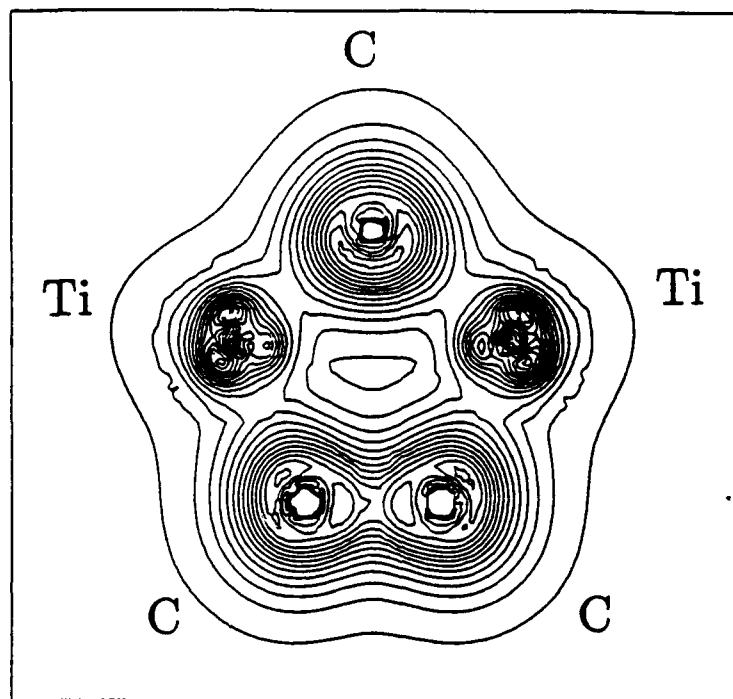
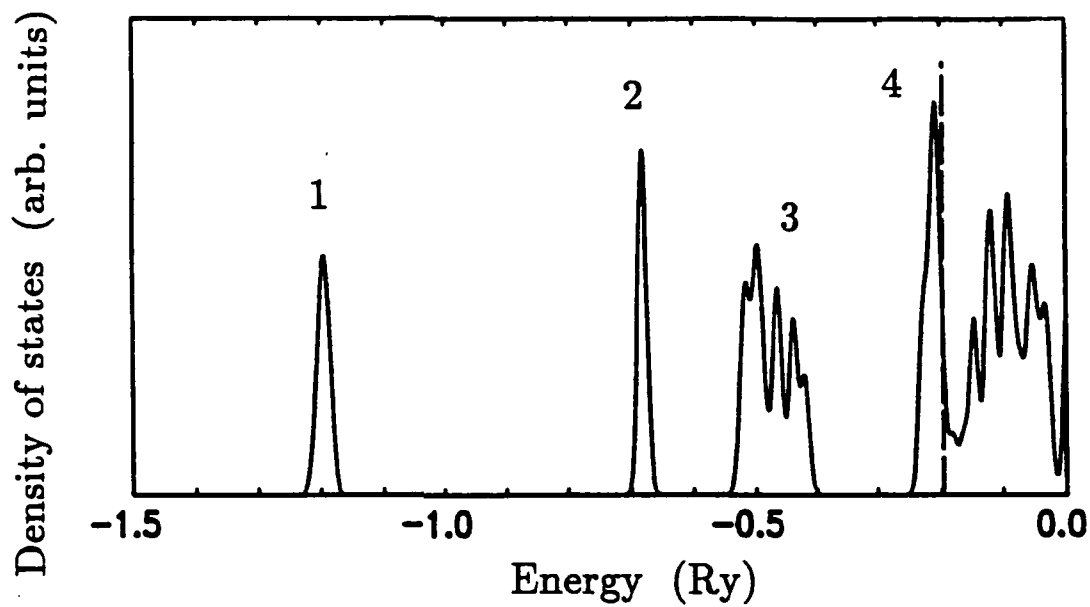


Fig. 2

PRL, Mettessal, Schilf, gonaric. Schilf



Ti atom

$3d \mid 4s \mid 4p$

C atom

$2s \mid$

$\mid 2p$

$C_2 \mid 1\sigma_g$

$1\sigma_u \mid$

$1\pi_u \parallel 2\sigma_g$

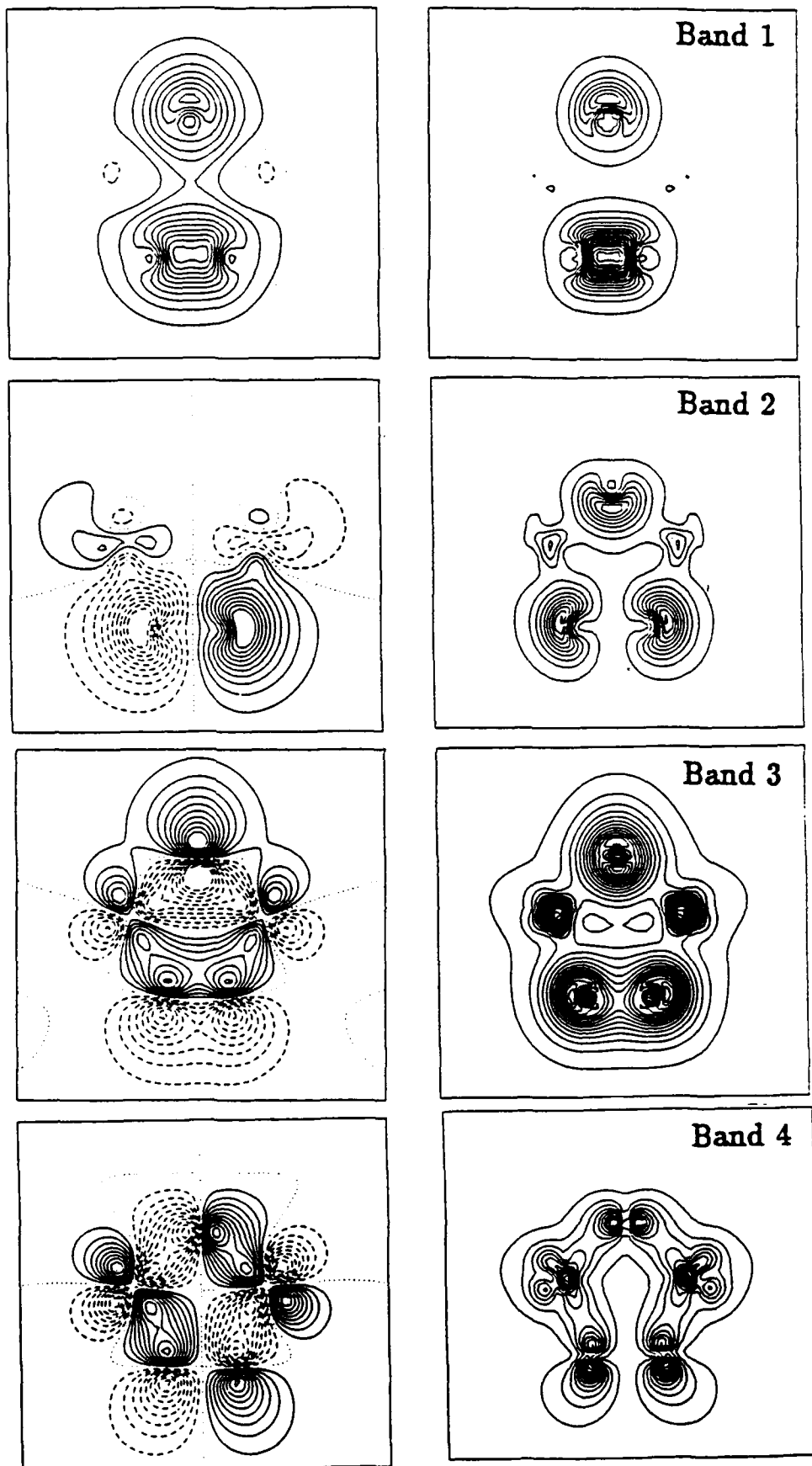
$1\pi_g \mid$

Fig. 3

PRL, Hoffmann, Schatzgorn, Schiffer



PRL,  
M. J. J. J.  
M. J. J. J.  
M. J. J. J.



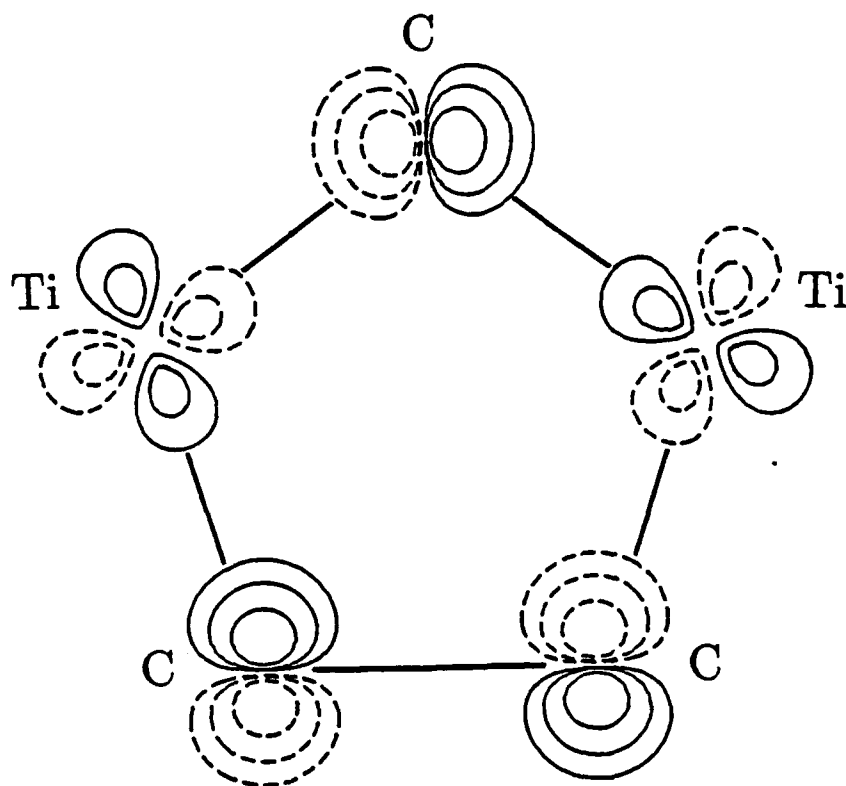


Fig. 5

PRL, Hoffmann, Schlegel, Hoffmann